Software implementation of the 3D-simulation procedure of SHS macrokinetics in the Ni-Al porous model medium with the closest packing of “mesocells”

V.I. Jordan[1,2], I.A. Shmakov[1], A.A. Grigorevskaya[1]

[1]Altai State University, Lenin avenue 61, Barnaul, Russia, 656049
[2] Khristianovich Institute of Theoretical and Applied Mechanics, Siberian Branch of RAS, Institutskaya str. 4/1, Novosibirsk, Russia, 630090

Abstract. The methodological features of the procedure for modeling the SHS macrokinetics in the model "etalon" structure of the densest packing of the so-called “mesocells” in the form of balls of the same radius are considered. In the center of the mesocell there is a spherical Ni particle (radius R_{Ni} = 30 μm), around which aluminum particles of radius R_{Al} = 10 μm are contained in a spherical interlayer with a thickness of 20 μm. The etalon structure is formed by a program that takes into account the distribution of mesocells in the structure of the closest packing (alternating flat layers with square symmetry). A technique for numerical solution of the heat conduction equation using an implicit scheme of bicyclic splitting based on the symmetric Krank-Nicholson scheme is implemented. Together with the bicyclic splitting scheme, a procedure is implemented for numerically solving the diffusion kinetics equation in mesocells. For computational speedup, the parallelization schemes of cycles are used, which determine the main time costs for performing "runs" in grid computing schemes.

1. Introduction

An effective method for producing modern materials with given properties is self-propagating high-temperature synthesis (SHS), during which an intense exothermic combustion reaction occurs in a small layer when exposed to a heat pulse on a mixture of fine-dispersed powders. A combustion wave propagates along the entire sample by heat transfer from layer to layer. The properties of SHS products largely depend on the initial structure of the particle packing of the reacting mixture and other reaction parameters (on the introduction of inert additives into the composition of the starting combustion reagents). In fact, the powder mixture is a porous spatially inhomogeneous medium with a specific structure of the packing of reagent particles. The authors of the article have at their disposal a program [1, 2] that generates the structure of particle packing from various materials (for example, Ni, Al particles, etc.) with different sizes and coordinates of filling the volume of the SHS sample mixture (with given statistical distributions). As shown by computational experiments on the generation of packing structures using this program, the average porosity of such structures (with spherical particles) practically turns out to be at least 40% (porosity from 40 to 70%). Such values of the porosity of the packing structure correspond to a greater extent to the so-called "packed (apparent) density" of the particles. The powder mixture subjected to external additional pressure (compression) reaches a lower level of porosity - 30% or less. Therefore, in order to obtain a denser packing structure as a “test” particle packing structure for testing the developed software package for studying the macrokinetics of

SH-synthesis, it was decided to implement a "test" closest packing structure with a high "symmetry" of particle arrangement and a relative filling density of the SHS sample volume at the level of 70% (porosity of about 30%). The aim of this work is to develop the algorithmic foundations and a software package for mathematical simulation and study of the macrokinetics of SH-synthesis of intermetallic compounds in binary systems such as Ni-Al and Ti-Al (taking into account discrete-continuous representations of the structure of the initial mixture and the structure of formation intermetallic phases in a reacting medium).

The system of equations of the SHS process consists of the heat equation (1) with the function of exothermic heat release (2) and the kinetics equation (3) with the kinetic function of homogeneous kinetics (4) for single-phase regions (Ni_3Al, NiAl, etc.).

$$\frac{\partial T}{\partial t} = \mathrm{div}\,(\alpha \cdot \mathrm{grad}(T)) + f(T,\eta), \tag{1}$$

$$f(T,\eta) = (Q/C_{уд}) \cdot k(T) \cdot \varphi(\eta) + \beta \cdot (T - T_0), \tag{2}$$

$$\frac{\partial \eta}{\partial t} = k(T) \cdot \varphi(\eta) = G(T,\eta), \tag{3}$$

$$\varphi(\eta) = (1-\eta)^n, \tag{4}$$

where $T = T(x, y, z, t)$ is the temperature at the current calculated spatial point of the mixture at time t; $\alpha=\lambda/(C_{уд}\cdot\rho)=\alpha(x, y, z, T)$ and $\lambda=\lambda(x, y, z, T)$ - respectively, thermal diffusivity and thermal conductivity of the mixture component; T_0 is the temperature of the environment; T_{ign} is the ignition temperature (self-ignition) of the SHS sample; $C_{уд}=c(x, y, z, T)$ and $\rho=\rho(x, y, z, T)$ - respectively, specific heat and density in the vicinity of the calculated point; $Q = Q(x, y, z, T)$ is the thermal effect of the reaction per unit mass of the product, taking into account stoichiometry of the composition of the components in the vicinity of the calculated point; $\eta=\eta(x, y, z, t)$ is the depth of the chemical transformation (mass fraction of the product relative to the mass of the reaction mixture and the product); β - coefficient taking into account heat loss to the environment.

It should be noted that often "in the first approximation" the temperature dependence of the parameters α, λ, c and ρ is neglected. However, for a wide range of temperature changes $T(x, y, z, t)$, such neglect is not justified and the approach proposed by the authors takes into account the inhomogeneity of thermophysical parameters and the discreteness of the porous medium.

Initial conditions (except for the boundary $z = 0$): $T(x, y, z, 0) = T_0$, at the boundary $z = 0$ at first $T(x, y, 0, 0) = T_{ign}$, and after a while - "free" boundary conditions of the first kind. The Arrhenius temperature-activation function has the form: $k(T) = k_0 \cdot \exp(-E/(R \cdot T))$, where k_0 is the pre-exponent and $E = E(x, y, z, T(x, y, z, t))$ is the reaction activation energy corresponding to the phase of the product.

2. Methodical features of SHS simulation procedure in the "etalon" model structure of the closest packing of mesocells

In this work, we use the "etalon" model structure of the closest packing (alternating flat layers with square symmetry, figure 1) of the so-called mesocells in the form of balls of the same radius (R_s = 50 μm), forming a regular structure in the form of a parallelepiped with certain properties symmetries of the arrangement of particles.

For convenience, figure 1 shows a fragment of a structure of three layers separated by Z coordinate, but in fact, these layers are closely adjacent to each other, i.e. a layer with an even number is superimposed in the wells of the underlying layer with an odd number (space filling factor 74.05%). In odd layers, the X- and Y-coordinates of the ball centers corresponding to each other coincide, and in the even layers, the X- and Y-coordinates of the ball centers are displaced in both coordinates relative to the balls of the odd layers by the radius of the ball R_s.

When testing the SHS simulation software package developed by the authors in the "etalon" model structure of the closest packing in odd layers, instead of 9 balls (3x3) are 36 balls (6x6), and in even layers instead of 4 balls (2x2) are 25 balls (5x5). Along the Z-coordinate, this structure contains 18 pairs of layers (18 alternating layers with odd and even numbers, respectively). As a result, the etalon

model structure (in the form of a parallelepiped) contains 1098 mesocells. In all layers in the central voids of each square of 4 balls, cubic structures of 8 aluminum balls of smaller radius R_{Al} = 10 μm are placed (two layers in the form of squares of 4 balls on top of each other). In addition, the structure of 1098 mesocells is additionally "truncated" by the lower horizontal and 4 lateral faces-planes passing through the centers of the lower 4 angular mesocell spheres and by the upper horizontal plane touching the mesocell spheres of the last 18th even layer. Thus, the dimensions of the reference structure along the X and Y axes are equal to 500 μm (from the center of the 1st to the center of the 6th ball), and about 2500 μm along the Z axis.

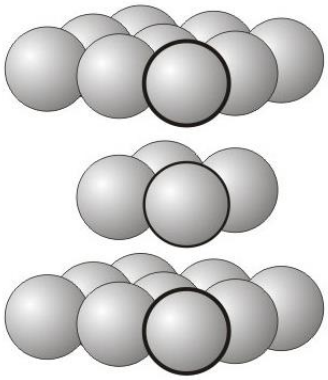

Figure 1. The closest cubic packing - flat layers with square symmetry [3].

To solve equations (1)-(4) using "grid" computational schemes (in this paper, based on Crank-Nicholson schemes), the procedure for preparing the "computational domain" in the form of a three-dimensional grid of nodal points with the same step h = 1 μm along the *x*, *y*, *z*-coordinates (the number of points is 625000000 = 500x500x2500). In a software package implemented in C ++ using the GCC-8 compiler, as well as using parallel programming systems OpenMP and MPICH 3.1.3 under the control of GNU/Linux, the data structure Points [*i*][*k*][*l*] with three fields has been created: Points[*i*][*k*][*l*].type; Points[*i*][*k*][*l*].*t*; Points[*i*][*k*][*l*].eta, where "type" is the type of material, *t* is the temperature, "eta" is the conversion level. These fields at each point of the Points [i] [k] [l] structure are used in current calculations and in each subsequent time layer (at each (*j*+1)-th iteration), at least the temperature and conversion level fields may are changed as a result of recalculation (the type of material at some iterations can also change).

Prior to the start of the SHS reaction, a spherical nickel particle Ni of radius R_{Ni} = 30 μm is located in the center of each mesocell of radius R_s = 50 μm, around which aluminum particles of radius R_{Al} = 10 μm are contained in the spherical interlayer (fig. 2a). In the course of the SHS reaction with increasing temperature in mesocells on the surfaces of central Ni particles, diffusion layers of intermetallic compounds are formed (fig. 2b), separating the Ni particle and the Al particle layer. Al particles at a temperature above the melting point of 933 K form a monolithic melt layer, as shown in figure 2b.

At each iteration in time (at the (*j*+1)-th iteration) for each spherical mesocell, the problem of diffusion kinetics [2] is solved, as a result of which the changed radii of intermetallic layers (Ni_3Al, NiAl, etc.) are fixed, which determine the estimated volumes of heat generation and which are used in the numerical solution of the heat equation using the implicit bicyclic splitting scheme based on the symmetric Crank-Nicholson scheme (see below).

The numerical solution of the problems of reaction diffusion in each mesocell is made independently of each other and therefore can be easily parallelized by independent computational processes (task parallelism). The following is a summary of the methodological features of the solution of the diffusion problem in the mesocell.

In each mesocell, the problem of diffusion kinetics is solved on the basis of a numerical solution of the diffusion equations and balance relations at moving interphase boundaries [4, 5]:

$$\frac{1}{D_i}\frac{\partial C_i}{\partial t} = \frac{\partial^2 C_i}{\partial r^2} + \frac{2}{r}\frac{\partial C_i}{\partial r}, \quad i=1, 2, \ldots, \tag{5}$$

$$r_i(t) \le r \le r_{i+1}(t),$$

$$r = r_i(t): \qquad (C_{i-1}^{+}(T) - C_i^{-}(T))\frac{\partial r_i}{\partial t} = -D_{i-1}(T)\frac{\partial C_{i-1}}{\partial r}\Big|_{r=r_i-0} + D_i(T)\frac{\partial C_i}{\partial r}\Big|_{r=r_i+0}, \qquad (6)$$

where C_i is the mass concentration of nickel in the i-th phase, $D_i(T) = k_i \exp(-E_i/(R \cdot T))$ is the mutual diffusion coefficient in the i-th layer, $C_{i-1}^{+}(T)$, $C_i^{-}(T)$ are the dependences of the equilibrium concentrations on temperature, given from state diagrams (boundaries of phase concentration regions). The number of layers (intermediate phases) depends on the type of system under consideration, therefore, the index i in the equations can take the values i = 2, 3, 4, 5, which corresponds to the phases: 1 - Ni, 2 - ε (Ni_3Al), 3 - δ (NiAl), 4 - γ (Ni_2Al_3), 5 - β ($NiAl_3$), 6 - Al. The radii of the phase layers are indicated as $r_i(t)$. Therefore, the radius $r_6 = R_s$.

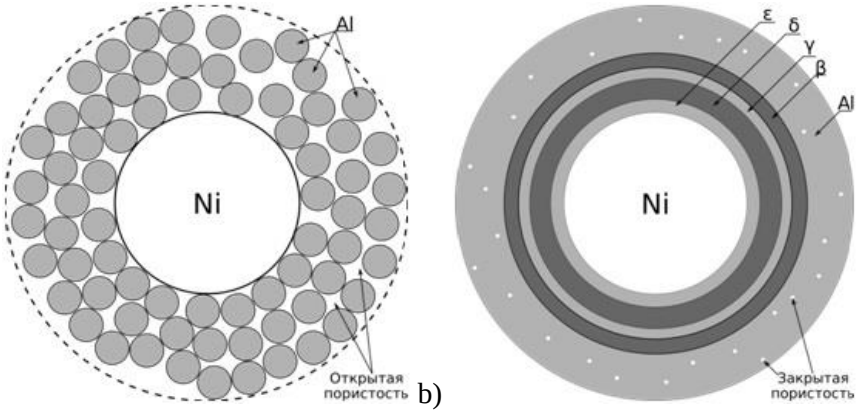

a) b)

Figure 2. Mesocell scheme: **(a)** before initiation of the SHS (T <933 K); **(b)** - in the process of SHS (T> 933 K); phases: ε - Ni_3Al, δ - NiAl, γ - Ni_2Al_3, β - $NiAl_3$.

Substituting in (6) the stationary solutions of equation (5): $C_i = A_i/r + B_i$, we obtain a system of ordinary differential equations [4]:

$$d_i \frac{\mathrm{d}r_i}{dt} = -\theta_{i-1}\frac{r_{i-1}}{r_i \cdot (r_i - r_{i-1})} + \theta_i \frac{r_{i+1}}{r_i \cdot (r_{i+1} - r_{i-1})}, \qquad (7)$$

where

$$d_i = C_{i-1}^{+}(T) - C_i^{-}(T), \quad \theta_i = D_i(T) \cdot (C_i^{+}(T) - C_i^{-}(T)), \ i = 1, 2, 3, 4.$$

Solving equations (7), for example, by the Runge-Kutta method, the radii of homogeneous phase layers (fig. 3b) are determined, which vary in time.

When solving the heat equation in phase interlayers, the kinetic function (4) of homogeneous kinetics is used. Then, in the temperature-activation function of Arrhenius $k(T) = k_0 \cdot \exp(-E/(R \cdot T))$ in each phase layer (with known restrictions on the radii r_{i-1} and r_i), we can take into account the corresponding constant k_0, activation energy E_i, etc. In addition, the temperature value corresponding to it, calculated when solving the heat equation, is taken into account in each phase layer. For each (j+1)-th moment of time t_{j+1} (for each (j+1)-th time layer) after calculating the values of the radii $r_i(t_{j+1})$, the temperature profile $T(x, y, z, t_{j+1})$ is calculated over the entire volume of the SHS-sample. The following is a procedure for solving the grid equations of heat conduction (1) and kinetics (3) in which grid schemes are obtained that correctly use the discontinuity property of the first kind of thermophysical and other parameters at the interfaces of different media (various particles).

In [6], an implicit bicyclic splitting scheme was derived based on the symmetric Crank – Nicholson scheme, which uses the separation ("splitting") of the time layer into 7 intermediate time layers and on the basis of which 8 equations are derived below. The first three equations (8)-(10), corresponding to the x, y, z- directions and simultaneously the i, k, l- indices, as well as the last three equations (14)-(16), corresponding in the opposite order to the z, y, x-directions and simultaneously the l, k, i-indices, are solved sequentially each time according to one of the three indicated indices by a one-dimensional

"sweep" method nested in 2-dimensional cycles according to the remaining indices. These 2-dimensional nested loops are fairly easy to parallelize.

$$A_{i,k,l}^{j+\frac{1}{2}} T_{i-1,k,l}^{j+\frac{1}{8}} - C_{i+1,k,l}^{j+\frac{1}{2}} T_{i,k,l}^{j+\frac{1}{8}} + B_{i+1,k,l}^{j+\frac{1}{2}} T_{i+1,k,l}^{j+\frac{1}{8}} = -F_{i+1,k,l}^{j}, \quad (8)$$

where $A_{i,k,l}^{j+\frac{1}{2}} = \frac{\tau}{4h^2}\alpha_{i,k,l}^{j+\frac{1}{2}}$; $C_{i+1,k,l}^{j+\frac{1}{2}} = \left[1+\left(\alpha_{i,k,l}^{j+\frac{1}{2}} + \alpha_{i+1,k,l}^{j+\frac{1}{2}}\right)\frac{\tau}{4h^2}\right]$; $B_{i+1,k,l}^{j+\frac{1}{2}} = \frac{\tau}{4h^2}\alpha_{i+1,k,l}^{j+\frac{1}{2}}$;

$F_{i+1,k,l}^{j} = A_{i,k,l}^{j+\frac{1}{2}} T_{i-1,k,l}^{j} + D_{i+1,k,l}^{j+\frac{1}{2}} T_{i,k,l}^{j} + B_{i+1,k,l}^{j+\frac{1}{2}} T_{i+1,k,l}^{j}$; $D_{i+1,k,l}^{j+\frac{1}{2}} = \left[1-\left(\alpha_{i,k,l}^{j+\frac{1}{2}} + \alpha_{i+1,k,l}^{j+\frac{1}{2}}\right)\frac{\tau}{4h^2}\right]$.

$$A_{i,k,l}^{j+\frac{1}{2}} T_{i,k-1,l}^{j+\frac{2}{8}} - C_{i,k+1,l}^{j+\frac{1}{2}} T_{i,k,l}^{j+\frac{2}{8}} + B_{i,k+1,l}^{j+\frac{1}{2}} T_{i,k+1,l}^{j+\frac{2}{8}} = -F_{i,k+1,l}^{j+\frac{1}{8}}, \quad (9)$$

where $A_{i,k,l}^{j+\frac{1}{2}} = \frac{\tau}{4h^2}\alpha_{i,k,l}^{j+\frac{1}{2}}$; $C_{i,k+1,l}^{j+\frac{1}{2}} = \left[1+\left(\alpha_{i,k,l}^{j+\frac{1}{2}} + \alpha_{i,k+1,l}^{j+\frac{1}{2}}\right)\frac{\tau}{4h^2}\right]$; $B_{i,k+1,l}^{j+\frac{1}{2}} = \frac{\tau}{4h^2}\alpha_{i,k+1,l}^{j+\frac{1}{2}}$;

$F_{i,k+1,l}^{j+\frac{1}{8}} = A_{i,k,l}^{j+\frac{1}{2}} T_{i,k-1,l}^{j+\frac{1}{8}} + D_{i,k+1,l}^{j+\frac{1}{2}} T_{i,k,l}^{j+\frac{1}{8}} + B_{i,k+1,l}^{j+\frac{1}{2}} T_{i,k+1,l}^{j+\frac{1}{8}}$; $D_{i,k+1,l}^{j+\frac{1}{2}} = \left[1-\left(\alpha_{i,k,l}^{j+\frac{1}{2}} + \alpha_{i,k+1,l}^{j+\frac{1}{2}}\right)\frac{\tau}{4h^2}\right]$.

$$A_{i,k,l}^{j+\frac{1}{2}} T_{i,k,l-1}^{j+\frac{3}{8}} - C_{i,k,l+1}^{j+\frac{1}{2}} T_{i,k,l}^{j+\frac{3}{8}} + B_{i,k,l+1}^{j+\frac{1}{2}} T_{i,k,l+1}^{j+\frac{3}{8}} = -F_{i,k,l+1}^{j+\frac{2}{8}}, \quad (10)$$

where $A_{i,k,l}^{j+\frac{1}{2}} = \frac{\tau}{4h^2}\alpha_{i,k,l}^{j+\frac{1}{2}}$; $C_{i,k,l+1}^{j+\frac{1}{2}} = \left[1+\left(\alpha_{i,k,l}^{j+\frac{1}{2}} + \alpha_{i,k,l+1}^{j+\frac{1}{2}}\right)\frac{\tau}{4h^2}\right]$; $B_{i,k,l+1}^{j+\frac{1}{2}} = \frac{\tau}{4h^2}\alpha_{i,k,l+1}^{j+\frac{1}{2}}$;

$F_{i,k,l+1}^{j+\frac{2}{8}} = A_{i,k,l}^{j+\frac{1}{2}} T_{i,k,l-1}^{j+\frac{2}{8}} + D_{i,k,l+1}^{j+\frac{1}{2}} T_{i,k,l}^{j+\frac{2}{8}} + B_{i,k,l+1}^{j+\frac{1}{2}} T_{i,k,l+1}^{j+\frac{2}{8}}$; $D_{i,k,l+1}^{j+\frac{1}{2}} = \left[1-\left(\alpha_{i,k,l}^{j+\frac{1}{2}} + \alpha_{i,k,l+1}^{j+\frac{1}{2}}\right)\frac{\tau}{4h^2}\right]$.

The equation of the fourth intermediate time layer of the circuit requires estimates $\hat{\eta}_{i,k,l}^{j+\frac{1}{2}}$ and $\hat{T}_{i,k,l}^{j+\frac{1}{2}}$, which can be obtained by a self-consistent cyclic process as follows.

We initialize $\hat{T}_{i,k,l}^{j+\frac{1}{2}} = T_{i,k,l}^{j+\frac{3}{8}}$. Then a self-consistency cycle is performed with a certain "threshold" for the accuracy of convergence of the estimates of the quantities $\hat{\eta}_{i,k,l}^{j+\frac{1}{2}}$ and $\hat{T}_{i,k,l}^{j+\frac{1}{2}}$ to their limiting values:

$$\left\{\hat{\eta}_{i,k,l}^{j+\frac{1}{2}} = \eta_{i,k,l}^{j} + \frac{\tau}{2}G\left(\hat{T}_{i,k,l}^{j+\frac{1}{2}}, \eta_{i,k,l}^{j}\right), \quad \hat{T}_{i,k,l}^{j+\frac{1}{2}} = T_{i,k,l}^{j+\frac{3}{8}} + \frac{\tau}{2}f\left(\hat{T}_{i,k,l}^{j+\frac{1}{2}}, \hat{\eta}_{i,k,l}^{j+\frac{1}{2}}\right)\right\}. \quad (11)$$

As a result of a certain number of iterations, estimates of $\hat{\eta}_{i,k,l}^{j+\frac{1}{2}}$ and $\hat{T}_{i,k,l}^{j+\frac{1}{2}}$ will be achieved with the necessary accuracy.

The equation of the fifth intermediate time layer of the circuit has the form:

$$T_{i,k,l}^{j+\frac{5}{8}} = T_{i,k,l}^{j+\frac{3}{8}} + \tau f\left(\hat{T}_{i,k,l}^{j+\frac{1}{2}}, \hat{\eta}_{i,k,l}^{j+\frac{1}{2}}\right). \quad (12)$$

The computational scheme for calculating the "conversion level" has the form:

$$\eta_{i,k,l}^{j+1} = \eta_{i,k,l}^{j} + \tau G\left(\hat{T}_{i,k,l}^{j+\frac{1}{2}}, \hat{\eta}_{i,k,l}^{j+\frac{1}{2}}\right). \quad (13)$$

Below are the schemes for the 6-th, 7-th intermediate layers in time and for the “final” (j+1)-th time layer.

$$A^{j+\frac{1}{2}}_{i,k,l}T^{j+\frac{6}{8}}_{i,k,l-1} - C^{j+\frac{1}{2}}_{i,k,l+1}T^{j+\frac{6}{8}}_{i,k,l} + B^{j+\frac{1}{2}}_{i,k,l+1}T^{j+\frac{6}{8}}_{i,k,l+1} = -F^{j+\frac{5}{8}}_{i,k,l+1}, \qquad (14)$$

where $A^{j+\frac{1}{2}}_{i,k,l} = \frac{\tau}{4h^2}\alpha^{j+\frac{1}{2}}_{i,k,l}$; $C^{j+\frac{1}{2}}_{i,k,l+1} = \left[1+\left(\alpha^{j+\frac{1}{2}}_{i,k,l} + \alpha^{j+\frac{1}{2}}_{i,k,l+1}\right)\frac{\tau}{4h^2}\right]$; $B^{j+\frac{1}{2}}_{i,k,l+1} = \frac{\tau}{4h^2}\alpha^{j+\frac{1}{2}}_{i,k,l+1}$;

$F^{j+\frac{5}{8}}_{i,k,l+1} = A^{j+\frac{1}{2}}_{i,k,l}T^{j+\frac{5}{8}}_{i,k,l-1} + D^{j+\frac{1}{2}}_{i,k,l+1}T^{j+\frac{5}{8}}_{i,k,l} + B^{j+\frac{1}{2}}_{i,k,l+1}T^{j+\frac{5}{8}}_{i,k,l+1}$; $D^{j+\frac{1}{2}}_{i,k,l+1} = \left[1-\left(\alpha^{j+\frac{1}{2}}_{i,k,l} + \alpha^{j+\frac{1}{2}}_{i,k,l+1}\right)\frac{\tau}{4h^2}\right]$.

The products of SHS are characterized by a variety of micro-, meso- and macrostructures, which

$$A^{j+\frac{1}{2}}_{i,k,l}T^{j+\frac{7}{8}}_{i,k-1,l} - C^{j+\frac{1}{2}}_{i,k+1,l}T^{j+\frac{7}{8}}_{i,k,l} + B^{j+\frac{1}{2}}_{i,k+1,l}T^{j+\frac{7}{8}}_{i,k+1,l} = -F^{j+\frac{6}{8}}_{i,k+1,l}, \qquad (15)$$

where $A^{j+\frac{1}{2}}_{i,k,l} = \frac{\tau}{4h^2}\alpha^{j+\frac{1}{2}}_{i,k,l}$; $C^{j+\frac{1}{2}}_{i,k+1,l} = \left[1+\left(\alpha^{j+\frac{1}{2}}_{i,k,l} + \alpha^{j+\frac{1}{2}}_{i,k+1,l}\right)\frac{\tau}{4h^2}\right]$; $B^{j+\frac{1}{2}}_{i,k+1,l} = \frac{\tau}{4h^2}\alpha^{j+\frac{1}{2}}_{i,k+1,l}$;

$F^{j+\frac{6}{8}}_{i,k+1,l} = A^{j+\frac{1}{2}}_{i,k,l}T^{j+\frac{6}{8}}_{i,k-1,l} + D^{j+\frac{1}{2}}_{i,k+1,l}T^{j+\frac{6}{8}}_{i,k,l} + B^{j+\frac{1}{2}}_{i,k+1,l}T^{j+\frac{6}{8}}_{i,k+1,l}$; $D^{j+\frac{1}{2}}_{i,k+1,l} = \left[1-\left(\alpha^{j+\frac{1}{2}}_{i,k,l} + \alpha^{j+\frac{1}{2}}_{i,k+1,l}\right)\frac{\tau}{4h^2}\right]$.

$$A^{j+\frac{1}{2}}_{i,k,l}T^{j+1}_{i-1,k,l} - C^{j+\frac{1}{2}}_{i+1,k,l}T^{j+1}_{i,k,l} + B^{j+\frac{1}{2}}_{i+1,k,l}T^{j+1}_{i+1,k,l} = -F^{j+\frac{7}{8}}_{i+1,k,l}, \qquad (16)$$

where $A^{j+\frac{1}{2}}_{i,k,l} = \frac{\tau}{4h^2}\alpha^{j+\frac{1}{2}}_{i,k,l}$; $C^{j+\frac{1}{2}}_{i+1,k,l} = \left[1+\left(\alpha^{j+\frac{1}{2}}_{i,k,l} + \alpha^{j+\frac{1}{2}}_{i+1,k,l}\right)\frac{\tau}{4h^2}\right]$; $B^{j+\frac{1}{2}}_{i+1,k,l} = \frac{\tau}{4h^2}\alpha^{j+\frac{1}{2}}_{i+1,k,l}$;

$F^{j+\frac{7}{8}}_{i+1,k,l} = A^{j+\frac{1}{2}}_{i,k,l}T^{j+\frac{7}{8}}_{i-1,k,l} + D^{j+\frac{1}{2}}_{i+1,k,l}T^{j+\frac{7}{8}}_{i,k,l} + B^{j+\frac{1}{2}}_{i+1,k,l}T^{j+\frac{7}{8}}_{i+1,k,l}$; $D^{j+\frac{1}{2}}_{i+1,k,l} = \left[1-\left(\alpha^{j+\frac{1}{2}}_{i,k,l} + \alpha^{j+\frac{1}{2}}_{i+1,k,l}\right)\frac{\tau}{4h^2}\right]$.

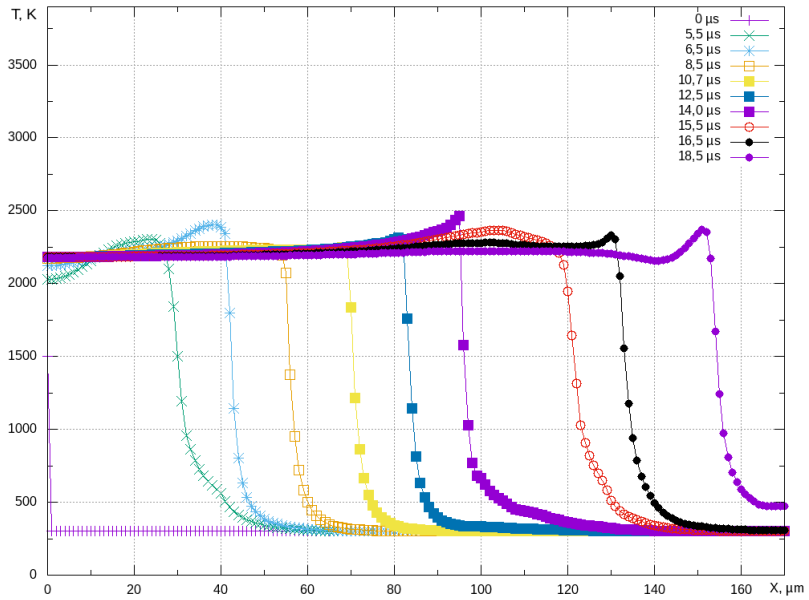

Figure 3. A set of temperature profiles (temperature distribution along the central direction of the SHS-sample) at different points in time: the initial temperature of the entire SHS sample is 300 K; the ignition temperature of the SHS-sample is 1500 K.

The following is an example of a test calculation of temperature profiles at different points in time (shown in figure 3) for a tightly packed mixture of particles (pore size less than 1 μm): the particle size

of Ni and Al is the same and equal to 1 μm. SHS initiation (ignition) mode: the initial temperature of the entire SHS mixture is 300 K; the ignition temperature of the SHS mixture is 1500 K. In a qualitative sense, the temperature profiles correspond to theoretical concepts. In addition, a super-adiabatic temperature difference is observed in the combustion front.

3. Conclusion

Computer simulation of SH-synthesis of intermetallic compounds of system Ni-Al by the software package using parallel computations was carried out on the cluster of workstations (15 PCs) - local area network. Each PC has a 4-core Intel i5-7400 processor, 4 GB RAM. Currently, the main assembly of the software package has been carried out, stability conditions for computational grid circuits have been determined, and test calculations have been carried out for the “etalon” model structure of the closest packing (alternating flat layers with square symmetry, fig. 1). During further testing, various parameters of the mathematical model of the SHS process will be refined to ensure agreement between the calculated data and experimental data from various literature sources.

4. Acknowledgments

The reported study was funded by RFBR according to the research projects No. 18-41-220004 and No. 18-08-01475.

5. References

[1] Jordan, V. 3D-Simulation of the Packing Structure of Spheroidal Particles in a Multicomponent Mixture by Molecular Dynamics / V. Jordan, A. Loktionov // Proceedings of Conference “Modeling of nonequilibrium systems” – Krasnoyarsk: “IPK SFU” Publisher, 2011. – P. 98-104.

[2] Jordan, V. Using the Mesoparticle Dynamics Method for 3D-Modeling of Packing Structures of Spheroidal Particles in Multicomponent Mixtures / V. Jordan, T. Belov // Proceedings of Conference “Information Technology and Mathematical Modeling” – Kemerovo: “Praktika” Publisher. – 2012. – Vol. 1. – P. 45-50.

[3] Closest packings [Electronic resource]. – Access mode: https://dic.academic.ru/dic.nsf/bse/143014/

[4] Kovalev, O. Mathematical Modeling of Metalchemical Reactions in a Two-Component Reactive Dispersed Mixture / O. Kovalev, V. Belyaev // Combustion, Explosion, and Shock Waves. – 2013. – Vol. 49(5). – P. 64-76.

[5] Jordan, V. Mathematical Simulation of the SH-Synthesis of Intermetallic Phases Taking into Account the Stationary Mode of Diffusion Kinetics in the "Mesocells" of the Periodic Structure of the Powder Mixture / V.I. Jordan, I.A. Shmakov, M.E. Kurgumbaev // Proceedings of Conference “Mathematics and its applications: fundamental problems of science and technology” – Barnaul: “AltGU” Publisher, 2015. – P. 264-272.

[6] Panchenko, Ju. Algorithmic bases and schemes of paralleling of calculations of macrokinetics of SHS taking into account discrete-continual representations of 3d-powder mixture / Ju. Panchenko, V. Jordan // High-Performance Computing Systems and Technologies. – 2018. – Vol. 2(2). – P. 54-62.